THE BELL SYSTEM TECHNICAL JOURNAL
Vol. 54, No. 1, January 1975
Printed in U.S.A.

Mode Coupling in an Optical Fiber With Core Distortions

By D. MARCUSE and H. M. PRESBY

(Manuscript received May 17, 1974)

The variations in the geometry of a step-index optical fiber are determined as functions of position along the axis of the fiber by an analysis of the backscattered light produced when a beam from a CW laser is incident perpendicular to the fiber axis. The power spectrum computed from this distortion function is then utilized with coupled-mode theory to predict the mode coupling, the reduction in pulse dispersion, and the accompanying increased radiation loss of the fiber. The theoretical calculations support experimental observations and account for a partial reduction in the multimode pulse dispersion.

I. INTRODUCTION

Optical-fiber communication systems utilizing incoherent light sources such as light-emitting diodes require the use of multimode waveguides to insure efficient excitation of the guide. Such guides, however, suffer from multimode pulse dispersion, because modes with higher group velocity arrive at the receiver earlier than modes with lower group velocity, limiting the information-carrying capacity of the fiber.

Thus, in a fiber of length L, uniform core of index n, uniform cladding of index $n\ (1 - \Delta)$, and constant cross section, a short pulse feeding equal amounts of power to every mode at the input will arrive at the other ends with a width $\tau = n\Delta L/c$, where c is the speed of light in free space.[1] For example, a fiber with $\Delta = 0.01$ and $n_2 = 1.5$ will have a delay spread of $\tau/L = 50$ ns/km, a serious limitation on either high-capacity or long-distance transmission.

Multimode pulse distortion can be reduced by introducing coupling between the guided modes.[2] The reduction in the pulse length comes about because some power traveling in a fast mode is eventually transferred to a slow mode, while power starting out in a slow mode finds

itself at least partially in a fast mode, so that the extremes of the group velocity spread are partly equalized. The root-mean-square delay spread is proportional to the square root of the product of fiber length L and the coupling length L_c associated with steady-state power transfer.[2] The multimode delay spread τ is thus reduced by a factor of $(L_c/L)^{\frac{1}{2}}$ which, in the case of strong coupling, $L_c \ll L$, can be significant.

One coupling mechanism that has been investigated in detail is geometric variations of the fiber along the longitudinal direction z.[3] If the deformation function $f(z)$, which is defined by these variations, is expanded in a Fourier series, two guided modes μ and ν with propagation constants β_μ and β_ν will be coupled by the Fourier component whose spatial frequency is given by[3] $\Omega = \beta_\mu - \beta_\nu$. In other words, the spatial period is the beat wavelength between the μth and νth modes. Using $n_1 = 1.5$ and $\Delta = 0.01$ as before and assuming a signal wavelength of 1.0 μm and a fiber core 50 μm wide, the beat wavelength for the adjacent lowest-order modes is 10 mm and for the adjacent modes near cut-off is 0.7 mm. Spatial periods greater than 10 mm will have very little effect on mode mixing and spatial periods less than 0.7 mm will create signal loss by coupling guided modes to the radiation field.

In this paper, the observation is reported of interface irregularities "unintentionally" introduced into a fiber during the pulling process. Distortions that are on the order of several microns are detected and measured by a backscattered light analysis technique. With the distortion function in hand, the power spectrum is computed and utilized to predict mode coupling, reduction in pulse dispersion, and accompanying increased radiation loss of the fiber. This represents the first time that the distortion function of a real fiber has actually been measured and utilized to predict transmission behavior.

II. EXPERIMENT

The fiber studied was pulled from a preform produced by a chemical vapor deposition (CVD) process.[4] The core of the fiber is elliptical, with major and minor axes on the order of 50 μm and 30 μm, respectively. The corresponding measurements for the outside fiber dimensions are 118 μm and 110 μm. A microinterferogram and a plot of the index profile are shown in Fig. 1. The profile is close to that of a step-index fiber with a very slight modification at the center. The maximum index difference between the core and the cladding is about $n_1 - n_2 = 0.0135$ or $\Delta = 0.0093$. It is important to point out that the refractive index profile did not vary by measurable amounts (less than one part in 10^4) over distances of interest for mode mixing in the fiber (0.2 cm to 2.0

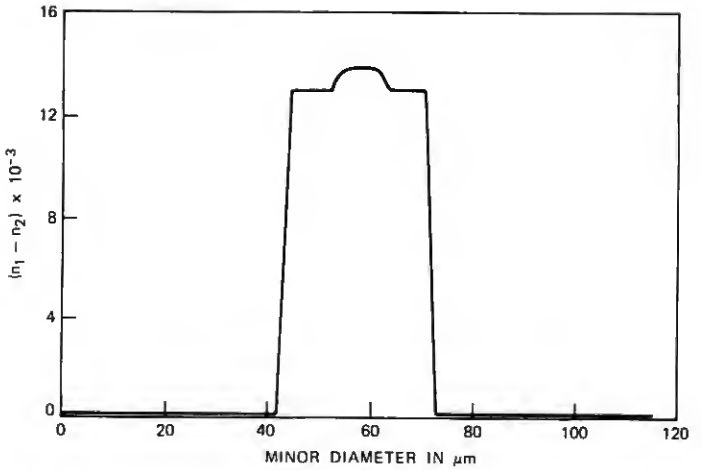

Fig. 1—Microinterferogram and index profile of CVD step-index fiber.

cm), though it did vary from one end of the 1-km fiber to the other.

If the geometry of the fiber remained uniform along its length as in Fig. 1, the fiber would propagate a given set of modes that would not couple among each other, producing a pulse spread of approximately 45 ns/km. The measured pulse width at the 10-dB point, however, was about 10 ns after nearly 1 km of fiber.[5]

To determine the core-cladding interface distortion, which we believe is at least partially responsible for this reduction in pulse dispersion, a backscattered light analysis technique was utilized.[6] This method can be used to detect the parameter b/a, where b is the radius of the fiber core and a is the radius of the cladding, assuming constant indexes of

refraction for the core and the cladding.[7] The technique has been extended to make observations on extended lengths of fiber by the set-up shown in Fig. 2. Light from a cw He-Ne laser is directed to oscillating mirror M_2 by means of fixed mirror M_1. The oscillating mirror serves to transform the ~1-mm circular beam into a line 1-mm wide, with length determined by the amplitude of oscillation. This line impinges upon the fiber, and the backscattered light is detected with photographic film.

A typical backscattered light distribution is shown in Fig. 3. Figure 3a is the overall pattern arising from a 12-cm length of fiber, and Fig. 3b is an expansion of the section on which measurements are made. The magnification in Fig. 3b is approximately 1 to 1. Figure 3a is symmetric about the midpoint with sharp cut-offs at the ends, typical of the backscattered light distribution.[6] As we go from the center of the pattern outward, we observe a region of enhanced fringe intensity. The location of the last fringe in this region is determined by the parameter b/a, assuming constant n_1 and n_2.[7] Here we interpret b and a as an average diameter. If the fiber were of uniform geometry along its length, the fringes would be straight parallel lines; the departure of this fringe from straightness gives a measure of the variation of b/a, and hence the distortion function of the fiber.

Measurements were made on several 14-cm lengths of fiber taken from both ends of the 1-km length. The appearance of the fringe dis-

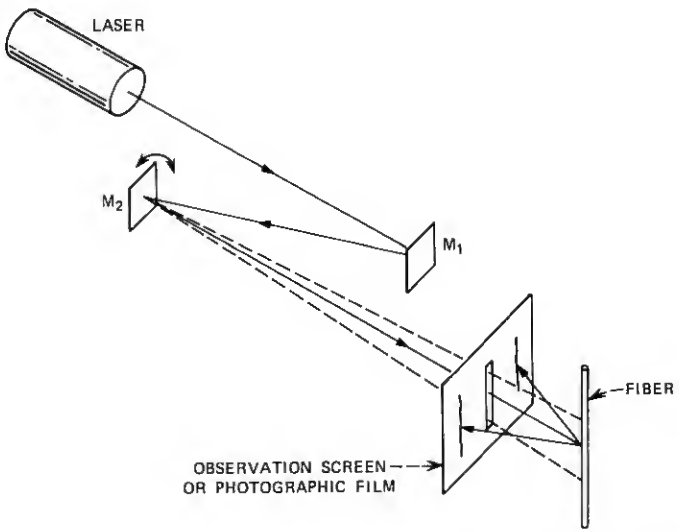

Fig. 2—Optical arrangement to determine core distortion function.

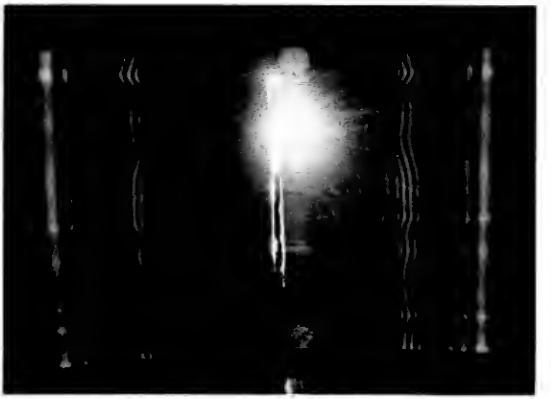

(a)

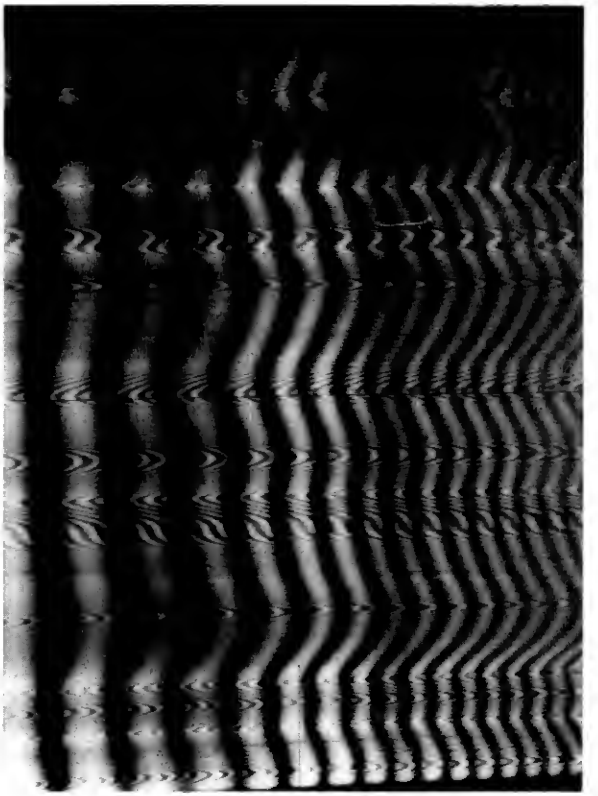

(b)

Fig. 3—Backscattered light patterns. (a) Complete pattern from 12.0-cm section of fiber. Slit in center allows for passage of incident light and bright spots in center are photographic artifacts. (b) Expansion of section of interest.

tortion was similar visually for other sections taken from intermediate portions of the fiber, but detailed measurements were not made on them. Figure 4 is a representative curve of the core distortion. The curve shows $\Delta b = f(z)$ plotted versus position along the fiber axis, with measurements made every 2 mm. The $f(z)$ variations are on the order of several percent.

We believe that the core-cladding interface distortions observed were introduced into the fiber during the pulling process. The preform was reduced to fiber form in an oxyhydrogen flame-pulling apparatus. Either the instability of the flame as a heat source or slight movements of the fiber because of air currents and back-flame effects or combinations of these are probably the contributing factors. Nonuniform pulling speeds and varying preform geometry may be additional factors, but they are expected to introduce variations with a much longer periodicity.

III. ANALYSIS

Given the core distortion function, the Fourier transform is then obtained by computer. A typical transform plot is shown as a bar

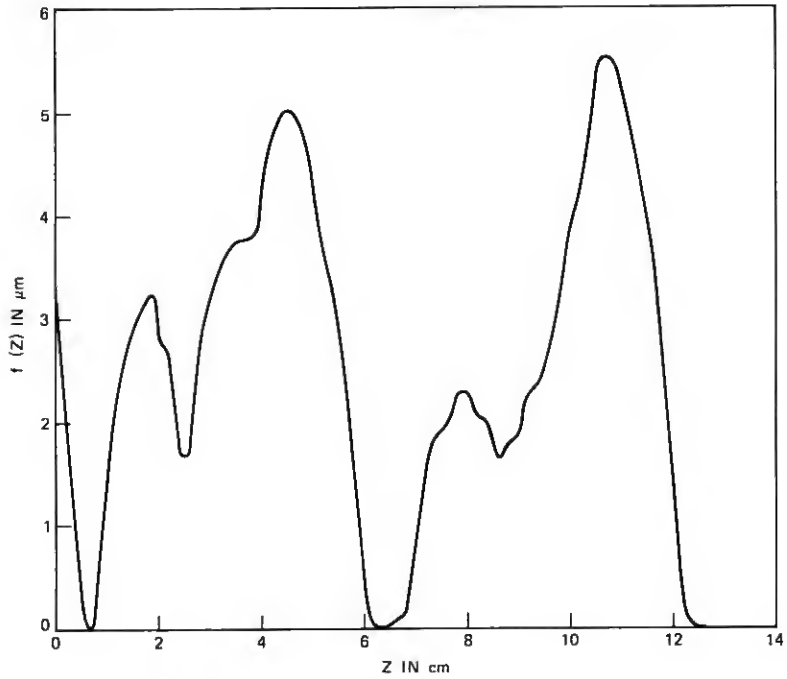

Fig. 4—Representative core distortion function.

graph in Fig. 5. We see that significant components exist in the coupling regions of interest. It is our aim to relate this spatial Fourier spectrum of the distortion function $f(z)$ to the pulse width reduction caused by mode coupling. The theory is described in detail in Ref. 8 for a fiber whose core maintains its circular cross section but is randomly bent. The core of the fiber examined in this paper has an elliptical cross section, and the observed variations consist of changes in the ellipticity. Modes of the elliptical fiber are very complicated and are difficult to apply to a mode-mixing analysis. For this reason, we simplify the problem by assuming that the fiber core nominally has a circular cross section that deforms itself randomly into an ellipse. It is assumed that this model is capable of yielding order-of-magnitude estimates of the performance of the actual fiber.

The core-cladding boundary r of a fiber with elliptical deformations can be described by the function[9]

$$r = b + f(z) \cos 2\phi. \tag{1}$$

The constant radius of the perfect fiber is b, $f(z)$ is the distortion function shown in Fig. 4 whose Fourier power spectrum is shown by the vertical bars in Fig. 5, and ϕ is the angle of the cylindrical coordinate system. A fiber with the core-cladding deformation of (1) couples modes according to the selection rule $\Delta\nu = \pm 2$.[3] The label ν, indicating the azimuthal mode number, enters the field expressions[3] via $\cos \nu\phi$ or $\sin \nu\phi$.

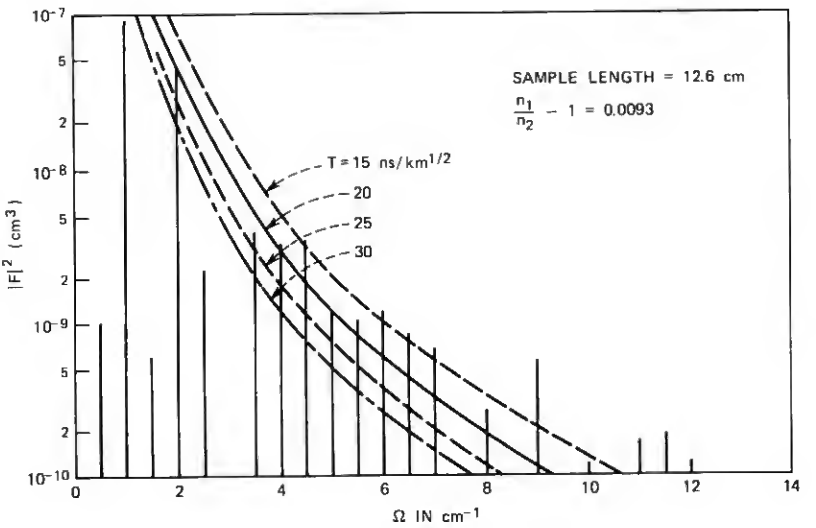

Fig. 5—Fourier transform of core distortion function.

If the power spectrum of $f(z)$ drops off sufficiently rapidly to limit mode coupling to nearest neighbors, the coupled power equations reduce to the form[10]

$$\frac{\partial P_{\nu,m}}{\partial z} = h_{\nu+2,m;\nu,m}(P_{\nu+2,m} - P_{\nu,m}) - h_{\nu,m;\nu-2,m}(P_{\nu,m} - P_{\nu-2,m}) + h_{\nu+2,m-1;\nu,m}(P_{\nu+2,m-1} - P_{\nu,m}) - h_{\nu,m;\nu-2,m+1}(P_{\nu m} - P_{\nu-2,m+1}). \quad (2)$$

$P_{\nu,m}$ is the average power carried by the mode labeled ν, m. In a crude approximation (applicable for small ν values and modes far from cutoff), the transverse propagation constant can be expressed as[11]

$$\kappa_{\nu,m} = (\nu + 2m)\frac{\pi}{2b}. \quad (3)$$

In addition to the already mentioned azimuthal mode number ν, we have also introduced the radial mode number m. Together, these two parameters form the compound mode number

$$M = \nu + 2m. \quad (4)$$

The expression in the second line on the right-hand side of (2) describes coupling among modes whose compound mode numbers differ by $\Delta M = 0$. In the crude model indicated by the approximation (3), modes with the same value of M have the same propagation constant and the same group velocity. This is not strictly true, since the degeneracy does not exist in the exact theory. However, the modes with the same M values are coupled very strongly, since coupling among them is caused by the large amplitudes at low spatial frequencies seen in Fig. 5. It is thus reasonable to assume that mode mixing among modes with identical values of M is so rapid that these modes carry equal amounts of power. This assumption causes the differences of the power with equal M values to disappear so that only the first line on the right-hand side of (2) remains. This coupling process is implicitly taken care of by requiring that modes with equal values of M carry identical amounts of power. Using the compound mode number, we write

$$P_{\nu,m} = P_M \quad P_{\nu+2,m} = P_{M+2} \quad P_{\nu-2,m} = P_{M-2} \quad (5)$$

$$h_{\nu+2,m;\nu m} = h_{M+2,M} \quad h_{\nu m;\nu-2,m} = h_{M,M-2}. \quad (6)$$

Equation (2) now assumes the form

$$\frac{\partial P_M}{\partial z} = h_{M+2,M}(P_{M+2} - P_M) - h_{M,M-2}(P_M - P_{M-2}). \quad (7)$$

We proceed by adding all equations of type (7) with the same value of M.[12] However, in addition to this simple summation we use the fact

that there are M modes with mode number M, but $M + 2$ modes with number $M + 2$. By replacing the differences occurring in (7) by differentials, we obtain

$$M \frac{\partial P_M}{\partial z} = 2(M + 2)h_{M+2,M} \frac{\partial P_{M+2}}{\partial M} - 2Mh_{M,M-2} \frac{\partial P_M}{\partial M}. \tag{8}$$

The replacement of the difference terms with derivatives is an approximation that is valid if there are very many guided modes, so that the M numbers are large and can be regarded as a quasi-continuum. With this approximation, (8) assumes the form

$$M \frac{\partial P_M}{\partial z} = 4 \frac{\partial}{\partial M} \left(Mh_M \frac{\partial P_M}{\partial M} \right). \tag{9}$$

We can express the compound mode number in terms of the cone angle θ, at which modes with the same values of M appear in the far-field radiation pattern that escapes from the end of the fiber.[3,12] Using[13]

$$M = \frac{2kb}{\pi} \theta \tag{10}$$

and

$$\frac{\partial \theta}{\partial M} = \frac{\pi}{2kb}, \tag{11}$$

with k = free space propagation constant and b = core radius, we obtain finally from (9) with $h_M = h = h(\theta)$

$$\frac{\partial P(z, \theta)}{\partial z} = \left(\frac{\pi}{kb} \right)^2 \frac{1}{\theta} \frac{\partial}{\partial \theta} \left(\theta h \frac{\partial P}{\partial \theta} \right). \tag{12}$$

The propagation of pulses is described by the time-dependent partial-differential equation

$$\frac{\partial P}{\partial z} + \frac{1}{v} \frac{\partial P}{\partial t} = \left(\frac{\pi}{kb} \right)^2 \frac{1}{\theta} \frac{\partial}{\partial \theta} \left(\theta h \frac{\partial P}{\partial \theta} \right), \tag{13}$$

where $v = v(\theta)$ is the group velocity of the mode labeled θ. Solutions to this equation are expressed in the form

$$P(z, t, \theta) = \sum_{j=1}^{N} \int_{-\infty}^{\infty} c_j(\omega) B(\omega, \theta) e^{-\rho^{(j)}(\omega) z} e^{i\omega t} d\omega. \tag{14}$$

The function $B_j(\omega, \theta)$ and the parameter $\rho^{(j)}(\omega)$ are obtained as solutions of an eigenvalue problem.[3] The eigenvalue $\rho^{(j)}$ is expanded into a perturbation series

$$\rho^{(j)}(\omega) = \sigma^{(j)} + \frac{i\omega}{v_a} + i\omega\rho_1^{(j)} + \omega^2 \rho_2^{(j)} + \cdots. \tag{15}$$

The second-order perturbation of the first eigenvalue, $\rho_2^{(1)}$, determines the width of the equilibrium pulse via the formula[14]

$$T = 4\sqrt{\rho_2^{(1)} L}, \tag{16}$$

where T is the full width of the gaussian-shaped impulse response of the multimode fiber measured between the $1/e$ points and L is the length of the fiber. It was assumed that the coupling coefficient h is independent of θ. This assumption corresponds to a spatial Fourier power spectrum of the distortion function $f(z)$ of the form

$$\langle |F(\theta)|^2 \rangle = \frac{C}{\Omega^4}. \tag{17}$$

Numerical differences between our present case and the example treated in Ref. 3 arise from the fact that the mode spacing (in β space) of nearest neighbors coupled by elliptical core deformations is twice as large as the spacing between nearest neighbors coupled by random bends. Taking these differences into account, we arrive at the following formula for the width of the equilibrium pulse:

$$T = \frac{1.26 n_2 [(n_1/n_2) - 1]^{\frac{1}{2}}}{c\sqrt{C}} \sqrt{L}, \tag{18}$$

in which n_1 and n_2 are the refractive indices of core and cladding, c is the velocity of light in vacuum, C is the constant defined in (17), and L is the length of the fiber.

For comparison with the length τ of a pulse carried by uncoupled modes, as mentioned earlier,

$$\tau = \frac{L}{c} n_2 \Delta, \tag{19}$$

we use the "improvement factor,"

$$R = \frac{T}{\tau} = \frac{1.26 \Delta^{\frac{1}{2}}}{\sqrt{CL}}, \tag{20}$$

with $\Delta = n_1/n_2 - 1$. The numerical values of R are physically meaningful only if $R < 1$. If $R > 1$, the guide length L or the coupling strength are too small for an equilibrium pulse to have established itself. The relative decrease of the pulse width achieved by mode coupling improves with increasing fiber length.

IV. DISCUSSION OF EXPERIMENTAL RESULTS

The step-index fiber used for this study exhibited unintentional, random fluctuations of the core-cladding boundary resulting in mode

coupling. According to (19), an uncoupled pulse width of $\tau = 45$ ns/km should have been observed for $\Delta = 9.3 \times 10^{-3}$; the actually observed pulse width was $\tau = 10$ ns/km. The observed core-cladding irregularities are able to account for a substantial part of the pulse shortening.

The function $f(z)$ of (1) is shown in Fig. 4 for a 12.6-cm section of the fiber. We consider the distortion of this fiber section as typical and representative of this particular fiber. The absolute square values of the Fourier components of the function shown in Fig. 4 are plotted in the bar graph of Fig. 5. It is clear that Fig. 5 does not represent the spatial power spectrum of the distortion function that enters the coupled-mode theory. The required power spectrum would have to be obtained by computing the Fourier spectrum of the function $f(z)$ for the entire length of the fiber. An approximation of this function could be obtained by computing Fourier spectra for a large number of shorter fiber sections and averaging. This procedure is time-consuming if it must be done manually, and an automated process would be required to determine the spatial Fourier spectra of the core-cladding interface distortion of the fiber.

In the absence of more information, we used the Fourier power spectrum shown in Fig. 5 to extract information about the mode coupling process. Since a theory based on a fourth-power law [see (17)] was already available, we approximated the data in Fig. 5 by fourth-power-law curves. The four curves plotted in the figure are possible approximations that may be roughly guessed from the bar graph. The numbers used to label the curves, $T = 15$, 20, 25, and 30 ns/km^4, are the result of determining the constant C of (17) from the curves and using it to calculate the width of the equilibrium pulse according to (18). Which of the four curves is the most plausible approximation to the actual Fourier power spectrum is open to discussion. It appears to us that the curves between $T = 20$ and $T = 25$ ns/km^4 seem to approximate the power spectrum reasonably well. The Fourier components for high spatial frequencies tend to exceed the values of the curves, while the curves are a little high for small spatial frequencies. Perhaps the fourth-order power law is not the best approximation to the Fourier power spectrum. On the other hand, we do not have enough information to obtain an accurate power spectrum. The high spatial frequencies shown in the bar graph result from rapid fluctuations of the curve $f(z)$ that are partly noise of the measurement process. It can thus be expected that the amplitudes of the high-frequency components appear exaggerated.

The most important point of this discussion is the observation that the measured core boundary distortions are indeed of the right order of magnitude to help explain the observed pulse shortening. Our data

can easily account for an improvement of the pulse width by $R = 0.5$. Since an improvement of $R = 0.2$ has been observed, it appears clear that the core boundary fluctuations are an important contributor to the observed pulse coupling behavior. The remaining amount of coupling may easily have been contributed by the bends of the fiber axis caused by the support mechanism and/or tension on the drum.[15]

Mode coupling with a fourth-power Fourier spectrum of (17) results in a loss penalty of[16]

$$R^2\sigma^{(1)}L = 0.5 \text{ dB}. \tag{21}$$

$\sigma^{(1)}$ is the steady-state loss coefficient resulting from mode mixing. For an $R = 0.5$, we thus expect an additional fiber loss of $\sigma^{(1)}L = 2$ dB. The observed pulse width improvement of $R = 0.2$ results in a loss penalty of $\sigma^{(1)}L = 10$ dB. The fiber losses actually observed are $\alpha = 30$ dB/km at a wavelength of 0.9 μm. The difference between these loss values is attributable to absorption losses in the fiber material.

The improvement factor R of (20) can be expressed in terms of a coupling length L_c,[2]

$$R = \left(\frac{L_c}{L}\right)^{\frac{1}{2}}. \tag{22}$$

For $R = 0.5$ we have $L_c = L/4$ or $L_c = 250$ m, since $L = 1$ km was assumed.

V. CONCLUSIONS

Mode coupling in multimode fibers may be caused by a number of fiber irregularities. Random index fluctuations, random bends, and core-cladding interface deformations are the most likely candidates. In this paper we have considered mode coupling by core-cladding interface deformations observed by a light-scattering technique that extracts the necessary information from the backscattered light of a laser that impinges on the fiber at right angles to its axis. The measured information was used to estimate the amount of pulse shortening that might be caused by this coupling mechanism. We found that the observed magnitude of the core-cladding boundary irregularities can explain some observed pulse shortening. The remainder may be caused by random bends introduced by the surface roughness of the drum on which the fiber is supported, or by refractive index changes along the fiber.

It appears that the backscattering technique used for the determination of the core-cladding interface irregularities may be a useful tool not only for monitoring the precision of fiber drawing processes but also for predicting the amount of mode coupling and consequently the pulse performance of multimode optical fibers. As shown here, to a

good degree this information can be extracted from a fiber only 12.6 cm long.

REFERENCES

1. S. E. Miller, E. A. J. Marcatili, and Tingye Li, "Research Towards Optical Fiber Transmission Systems," Proc. IEEE, *61*, No. 12 (December 1973), pp. 1703–1751.
2. S. D. Personick, "Time Dispersion in Dielectric Waveguides," B.S.T.J., *50*, No. 3 (March 1971), pp. 843–859.
3. D. Marcuse, "Theory of Dielectric Optical Waveguides," New York: Academic Press, 1974.
4. J. B. MacChesney, P. B. O'Connor, J. Simpson, and F. V. DiMarcello, "Multimode Optical Wave Guides Having a Vapor Deposited Core of Germania Doped Borosilicate Glass," Ceramic Bulletin Paper 31-6-73F, *52*, No. 9 (September 1973), p. 704.
5. L. G. Cohen, unpublished data.
6. H. M. Presby, "Refractive Index and Diameter Measurements of Unclad Optical Fibers," J. Opt. Soc. Am. *64*, No. 3 (March 1974), pp. 280–284.
7. H. M. Presby and D. Marcuse, "Refractive Index and Diameter Measurements of Step-Index Optical Fibers and Preforms," to be published in Appl. Opt., Dec. 1974.
8. Ref. 3, Section 5.6.
9. Ref. 3, Eq. (3.6-1).
10. Ref. 3, Eq. (5.2-19).
11. Ref. 3, Eqs. (2.2-10) and (2.2.71).
12. D. Gloge, "Optical Power Flow in Multimode Fibers," B.S.T.J., *51*, No. 8 (October 1972), pp. 1767–1783.
13. Ref. 3, Eq. (5.6-12).
14. Ref. 3, Eq. (5.5-25).
15. D. B. Keck, "Observation of Externally Controlled Mode Coupling in Optical Waveguide," Proc. IEEE, *62*, No. 5 (May 1974), pp. 649–650.
16. Ref. 3, Eq. (5.6-66).